On the Maxwell−Stefan Approach to Diffusion: A General Resolution in the Transient Regime for One-Dimensional Systems

Erminia Leonardi*,† and Celestino Angeli‡

CRS4, Center for Advanced Studies, Research and Development in Sardinia, Parco Scientifico e Tecnologico, Polaris, Edificio 1, I-09010 Pula, Italy, and Dipartimento di Chimica, Università di Ferrara, Via Borsari 46, I-44100 Ferrara, Italy

Received: January 26, 2009; Revised Manuscript Received: October 13, 2009

The diffusion process in a multicomponent system can be formulated in a general form by the generalized Maxwell−Stefan equations. This formulation is able to describe the diffusion process in different systems, such as, for instance, bulk diffusion (in the gas, liquid, and solid phase) and diffusion in microporous materials (membranes, zeolites, nanotubes, etc.). The Maxwell−Stefan equations can be solved analytically (only in special cases) or by numerical approaches. Different numerical strategies have been previously presented, but the number of diffusing species is normally restricted, with only few exceptions, to three in bulk diffusion and to two in microporous systems, unless simplifications of the Maxwell−Stefan equations are considered. In the literature, a large effort has been devoted to the derivation of the analytic expression of the elements of the Fick-like diffusion matrix and therefore to the symbolic inversion of a square matrix with dimensions $n \times n$ (n being the number of independent components). This step, which can be easily performed for $n = 2$ and remains reasonable for $n = 3$, becomes rapidly very complex in problems with a large number of components. This paper addresses the problem of the numerical resolution of the Maxwell−Stefan equations in the transient regime for a one-dimensional system with a generic number of components, avoiding the definition of the analytic expression of the elements of the Fick-like diffusion matrix. To this aim, two approaches have been implemented in a computational code; the first is the simple finite difference second-order accurate in time Crank−Nicolson scheme for which the full mathematical derivation and the relevant final equations are reported. The second is based on the more accurate backward differentiation formulas, BDF, or Gear's method (Shampine, L. F.; Gear, C. W. *SIAM Rev.* **1979**, *21*, 1.), as implemented in the Livermore solver for ordinary differential equations, LSODE (Hindmarsh, A. C. *Serial Fortran Solvers for ODE Initial Value Problems*, Technical Report; https://computation.llnl.gov/casc/odepack/odepack_ home.html (**2006**).). Both methods have been applied to a series of specific problems, such as bulk diffusion of acetone and methanol through stagnant air, uptake of two components on a microporous material in a model system, and permeation across a microporous membrane in model systems, both with the aim to validate the method and to add new information to the comprehension of the peculiar behavior of these systems. The approach is validated by comparison with different published results and with analytic expressions for the steady-state concentration profiles or fluxes in particular systems. The possibility to treat a generic number of components (the limitation being essentially the computational power) is also tested, and results are reported on the permeation of a five component mixture through a membrane in a model system. It is worth noticing that the algorithm here reported can be applied also to the Fick formulation of the diffusion problem with concentration-dependent diffusion coefficients.

Introduction

The description, interpretation, modeling, and simulation of the multicomponent diffusion process is a crucial aspect in many research and industrial activities. For this reason, it is the subject of a large number of books and reviews, as well as an active research field. An overview of the different theoretical approaches to diffusion is beyond the scope of this paper. We restrict ourselves to remind that multicomponent diffusion can be described essentially within three strategies. In the following, a short summary of these approaches is reported; the reader is referred to recent reviews for more details.[3−6] Moreover, the attention is focused on one-dimensional systems (z being the considered coordinate), given that this is the subject of the present work.

The first approach is known as the Fick law of diffusion; the molar flux of component i, N_i, is written as a linear combination of the concentration gradients, dc_j/dz, of all components

$$N_i = -\sum_{j=1}^{n} D_{ij}\frac{dc_j}{dz} \tag{1}$$

This formulation is phenomenological; the diffusion coefficients, D_{ij}, are obtained from experiments and can show a marked dependence on the concentrations. An example can be found in a work of Krishna and Wesselingh,[3] where an analysis of an experimental study reported by Duncan and Toor[7] in 1962 on an ideal ternary gas mixture indicates a curious behavior for

* To whom correspondence should be addressed. E-mail: ermy@crs4.it.
† Parco Scientifico e Tecnologico.
‡ Università di Ferrara.

10.1021/jp900760c
Published on Web 12/14/2009

one component. Here (and in the following), "concentration" has a general meaning and indicates different quantities following the problem under study (for instance, it can be a partial pressure in the case of a gas mixture or a fractional occupancy for surface diffusion in microporous materials).

The second approach is based on irreversible thermodynamics. In this case, N_i is a linear combination of the chemical potential gradients, $d\mu_j/dz$, which are the driving forces for diffusion:

$$N_i = -\sum_{j=1}^{n} L_{ij}\frac{d\mu_j}{dz} \tag{2}$$

The elements L_{ij} are called Onsager phenomenological coefficients and satisfy the reciprocal relation, $L_{ij} = L_{ji}$.

Finally, the third approach is due to Maxwell[8] and Stefan[9] (MS) and is based on a microscopic hypothesis on the physical effects controlling the diffusion process. In this formulation, as clearly reported by Krishna and Wasselingh,[3] two forces are exerted on the *i* molecules, and these two forces cancel out each other. The first force is the chemical potential gradient, $-d\mu_i/dz$, and it is the driving force for diffusion. This force is counterbalanced by the friction with all of the other moving species *j*; this friction is proportional to the differences between the velocities of the two species and to the concentration of *j*. The proportionality coefficient is written as $1/Đ_{ij}$, where the $Đ_{ij}$ are called MS diffusivities and represent the inverse of a drag coefficient. After some algebraic manipulation, the MS equations can be cast in the form

$$-\frac{x_i}{RT}\frac{d\mu_i}{dz} = \sum_{j=1,j\neq i}^{n}\frac{x_jN_i - x_iN_j}{c_tĐ_{ij}} \tag{3}$$

where $x_i = c_i/c_t$ are the molar fractions (c_t being the total molar concentration).

One can show that the three formulations are actually fully equivalent (as reported by different authors; see Wang and LeVan[10] for a recent and complete analysis) and that simple equations relate the three key quantities, the Fick diffusivities, the phenomenological Onsager coefficients, and the MS diffusivities. These three approaches can be further connected to other theories (see, for instance, Mitrovic[11] for a derivation of the MS equations from the classical Lagrange equations).

Among the different approaches, the MS formulation has gained in the last decades a central position, in particular for the description of the multicomponent diffusion process in microporous systems. Many technologically relevant processes fall into this category; to report only a few examples, let us cite diffusion in microporous membranes,[6] pressure swing adsorption,[12] diffusion in carbon nanotubes,[13] capillary diffusion,[14] remediation of contaminated groundwater,[15,16] membrane electrolysis process,[17] gas transport in porous fuel cell anodes,[18,19] enantiomer separation in chromatography,[20] and membrane distillation.[21]

Moreover, the MS equations are used to describe the diffusion, besides in "standard" gas and liquid phases, in more extreme situations, such as, for instance, in high-temperature gas nuclear reactors[22] and in plasma mixtures.[23,24]

The MS equations can be solved analytically (only in special cases[25−27]) or by numerical approaches. The theoretical description of the physical systems reported above requires a general and stable numerical method able to solve the MS equations in the transient regime for a generic number of components without introducing approximations (apart, obviously, from those of the numerical procedure). Moreover, a remarkable strong point would be the possibility to manage the various choice for what concerns, for instance, the MS diffusivities (constant or dependent on the concentrations), the adsorption isotherm (for microporous material), and other physical parameters, allowing one to treat all of these systems, described with different physical models, within a unique computational tool.

The aim of this paper is to present such a tool, from the definition of the numerical algorithm, to its implementation in a computational code, and finally, to its application on actual problems.

The remainder of the paper is organized as follows; in the next sections the MS equations are discussed for the diffusion in different physical systems, the numerical algorithm is presented, the method is validated by comparison with previously published results, and new applications are reported. Finally, the Conclusions section presents some conclusive remarks.

The Generalized Maxwell−Stefan Equations

The generalized MS equations[8,9] (for a general review, the reader is referred to Krishna and Wesselingh[3]) describe the mass transfer process in a multicomponent system by relating the molar fluxes, N_i, with the chemical potential gradients, $d\mu_i/dz$. These equations can be cast in different forms, following the nature of the system under consideration. Hereafter, three cases are reported in details.

Diffusion within a Bulk Fluid Phase. For the diffusion within a bulk fluid phase,[3] one has

$$-\frac{x_i}{RT}\frac{d\mu_i}{dz} = \sum_{j=1,j\neq i}^{n}\frac{x_jN_i - x_iN_j}{c_tĐ_{ij}} \tag{4}$$

It is worth noticing that only $n - 1$ of these equations are independent due to the Gibbs−Duhem equation

$$\sum_{i=1}^{n} x_i\nabla_T\mu_i = \nabla p \tag{5}$$

By using the relation

$$\frac{d\mu_i}{dz} = \sum_{j=1}^{n-1}\frac{\partial\mu_i}{\partial x_j}\frac{\partial x_j}{\partial z} \tag{6}$$

the left-hand side of eq 4 can be written as

$$-\frac{x_i}{RT}\frac{d\mu_i}{dz} = -\sum_{j=1}^{n-1}\Gamma_{ij}\frac{\partial x_j}{\partial z} \tag{7}$$

where the $(n - 1) \times (n - 1)$ matrix of thermodynamic factors, Γ, has been introduced. It has elements

$$\Gamma_{ij} = \frac{x_i}{RT}\frac{\partial\mu_i}{\partial x_j} = \delta_{ij} + x_i\frac{\partial \ln\gamma_i}{\partial x_j} \tag{8}$$

where γ_i are the activity coefficients. Let us note that for an ideal gas mixture, $\Gamma_{ij} = \delta_{ij}$.

In the case of equimolar diffusion (no net transfer flux out or into the system), one has

$$N_t = \sum_i^n N_i = 0 \tag{9}$$

that is

$$N_n = -\sum_i^{n-1} N_i \tag{10}$$

Substituting this expression into eq 4, the right-hand side of it can be put in the matrix form c_t^{-1}BN, where the vector N collects the first $n - 1$ fluxes and the $(n - 1) \times (n - 1)$ B matrix has elements

$$B_{ii} = \frac{x_i}{Đ_{in}} + \sum_{k=1,k\neq i}^{n} \frac{x_k}{Đ_{ik}} \tag{11}$$

and

$$B_{ij} = -x_i\left(\frac{1}{Đ_{ij}} - \frac{1}{Đ_{in}}\right) \qquad i \neq j \tag{12}$$

With these definitions, eq 4 becomes

$$-c_t\Gamma\left(\frac{\partial x}{\partial z}\right) = \mathrm{BN} \tag{13}$$

where the vector $(\partial x/\partial z)$ collects the first $n - 1$ molar fraction gradients $\partial x_i/\partial z$.

Finally, the fluxes are obtained by the relation

$$\mathrm{N} = -c_t\mathrm{B}^{-1}\Gamma\left(\frac{\partial x}{\partial z}\right) = -c_t\mathrm{D}\left(\frac{\partial x}{\partial z}\right) \tag{14}$$

with

$$\mathrm{D} = \mathrm{B}^{-1}\Gamma \tag{15}$$

A special type of bulk diffusion is the case where one of the components is stagnant. An example of this process is the experimental study of Carty and Schrodt,[25] considered in detail in this work.

For such a process, eq 9 is replaced by the condition $N_n = 0$ (for simplicity, the stagnant component is considered to be the last one). The only modification with respect to equimolar diffusion concerns the B matrix, which assumes the form

$$B_{ii} = \sum_{k=1,k\neq i}^{n} \frac{x_k}{Đ_{ik}} \tag{16}$$

and

$$B_{ij} = -\frac{x_i}{Đ_{ij}} \tag{17}$$

Diffusion within Macropores: The Dusty Gas Model. In the diffusion of a mixture within macropores, two transport mechanisms are dominant,[28] the free molecular (bulk) diffusion, when intermolecular collisions dominate over molecule−wall collisions, and the Knudsen diffusion, when molecule−wall collisions dominates over intermolecular collisions. The first mechanism is more important for large pore sizes and high system pressure, while for small pore sizes and low system pressure, the second dominates. However, both processes must be normally taken into account because in many systems, both occur.

In this case, the MS equations are

$$-\frac{x_i}{RT}\frac{\mathrm{d}\mu_i}{\mathrm{d}z} = \sum_{j=1,j\neq i}^{n} \frac{x_jN_i - x_iN_j}{c_tĐ_{ij}} + \frac{N_i}{Đ_{i,\mathrm{Kn}}} \tag{18}$$

where $Đ_{i,\mathrm{Kn}}$ is the Knudsen diffusivity of species i.[28]

For an ideal gas mixture ($\Gamma = 1$), these equations can be cast in the form

$$\mathrm{N} = -c_t\mathrm{D}\left(\frac{\partial x}{\partial z}\right) \qquad \mathrm{D} = \mathrm{B}^{-1} \tag{19}$$

where N is a vector collecting the fluxes of the n components and the $(n \times n)$ B matrix has elements

$$B_{ii} = \frac{1}{Đ_{i,\mathrm{Kn}}} + \sum_{k=1,k\neq i}^{n} \frac{x_k}{Đ_{ik}} \tag{20}$$

and

$$B_{ij} = -\frac{x_i}{Đ_{ij}} \tag{21}$$

Diffusion within Micropores. In the case of diffusion within micropores, the diffusing molecules always feel the force field of the pore surfaces; therefore, the process is assimilated to a surface diffusion. In this situation, the MS equations are written as[29]

$$-\rho\frac{\theta_i}{RT}\frac{\mathrm{d}\mu_i}{\mathrm{d}z} = \sum_{j=1,j\neq i}^{n} \frac{q_jN_i^s - q_iN_j^s}{q_i^{\mathrm{sat}}q_j^{\mathrm{sat}}Đ_{ij}^s} + \frac{N_i^s}{q_i^{\mathrm{sat}}Đ_i^s} \tag{22}$$

where N_i^s are the surface fluxes, q_i is the loading of component i (in molecules per unit cell or mol kg^{-1}), q_i^{sat} is the saturation loading of component i, $\theta_i = q_i/q_i^{\mathrm{sat}}$ are the fractional occupancies of the surface sites (also called coverages), and ρ is the density (in number of unit cell per m^3 or kg m^{-3}).

The final relevant equations, in this case, are

$$\mathrm{N}^s = -\rho\mathrm{D}\left(\frac{\partial\theta}{\partial z}\right) \tag{23}$$

$$\mathrm{D} = \mathrm{q}^{\mathrm{sat}}\mathrm{B}^{-1}\Gamma \tag{24}$$

where $\mathrm{q}^{\mathrm{sat}}$ is a diagonal matrix with the q_i^{sat} as diagonal elements and the matrix B is defined by

$$B_{ii} = \frac{1}{Đ_i^s} + \sum_{k=1,k\neq i}^{n} \frac{\theta_k}{Đ_{ik}^s} \tag{25}$$

and

$$B_{ij} = -\frac{\theta_i}{Đ_{ij}^{s}} \tag{26}$$

The expression of the Γ matrix elements depends on the adsorption isotherm of the microporous system. In the simplest case, the Langmuir isotherm with equal saturation loadings, one has

$$\Gamma_{ij} = \delta_{ij} + \frac{\theta_i}{\theta_V} \tag{27}$$

where $\theta_V = 1 - \sum_{i=1}^{n} \theta_i$ is the fraction of unoccupied sites.

Numerical Resolution of the Maxwell−Stefan Equations

It is worth noticing that in all cases discussed in the last section, the MS equations can be reformulated in a Fick-like expression, where the vector of the fluxes is equal (apart from a constant) to the product of a matrix D and the vector collecting the concentration gradients.

The continuity equation for component *i*, in the case of the diffusion within a bulk fluid phase in one dimension system, is

$$c_t \frac{\partial x_i}{\partial t} = -\frac{\partial N_i}{\partial z} \tag{28}$$

Using eq 14 for the flux, eq 28 can written as

$$\frac{\partial x_i}{\partial t} = \frac{\partial}{\partial z}\left[\mathrm{D}\left(\frac{\partial x}{\partial z}\right)\right]_i = \sum_{i'=1}^{n-1} \frac{\partial}{\partial z}\left[D_{ii'}\frac{\partial x_{i'}}{\partial z}\right] \tag{29}$$

These equations are coupled and form a system of nonlinear second-order parabolic partial differential equations (PDEs).

While in the Fick formulation of diffusion the matrix D is often considered constant, thus simplifying the resolution of the system of PDEs (eq 29), in the MS approach, this is a drastic approximation. The dependence of the elements of the D matrix (through the B^{-1} and Γ matrices) on the unknown concentration is complex; it can be easily derived in an analytic form for the case of two independent components, as reported in various papers,[29,30] and it remains an affordable task for three[31] and perhaps four independent components. As an example, in the case of the membrane permeation of a two-component mixture, from eqs 23−25, one can eventually obtain the analytic expression of the fluxes[29]

$$N_1^{s} = -\rho \frac{q_1^{sat} Đ_1 \left[\left\{\Gamma_{11} + \theta_1 \frac{Đ_2}{Đ_{12}}(\Gamma_{11} + \Gamma_{21})\right\}\frac{\partial \theta_1}{\partial z} + \left\{\Gamma_{12} + \theta_1 \frac{Đ_2}{Đ_{12}}(\Gamma_{12} + \Gamma_{22})\right\}\frac{\partial \theta_2}{\partial z}\right]}{\theta_2 \frac{Đ_1}{Đ_{12}} + \theta_1 \frac{Đ_2}{Đ_{12}} + 1} \tag{30}$$

$$N_1^{s} = -\rho \frac{q_2^{sat} Đ_2 \left[\left\{\Gamma_{22} + \theta_2 \frac{Đ_1}{Đ_{12}}(\Gamma_{22} + \Gamma_{12})\right\}\frac{\partial \theta_2}{\partial z} + \left\{\Gamma_{21} + \theta_2 \frac{Đ_1}{Đ_{12}}(\Gamma_{21} + \Gamma_{11})\right\}\frac{\partial \theta_1}{\partial z}\right]}{\theta_2 \frac{Đ_1}{Đ_{12}} + \theta_1 \frac{Đ_2}{Đ_{12}} + 1} \tag{31}$$

For a number of independent components beyond four, the derivation of the analytic expression of the D matrix elements becomes rapidly too complex.

Even if the analytic expression of D is known, one has to deal with the problem of the dependence of D on the unknown concentration (and therefore on the position), a relevant aspect for the numerical resolution of the system of PDEs (29). This point can be faced by using very efficient computer packages implementing numerical schemes of different quality; in the finite difference scheme, the problem can be solved with the method of lines[32] using the semi-implicit Runge−Kutta methods (such as, for instance, the Crank−Nicolson[33,34] approach) or the more refined multistep methods (as, for instance, the backward differentiation formulas, BDF, or Gear's method[1]). One can also cite other approaches as, for instance, the orthogonal collocation on the finite element[35] algorithm coupled with ODE solvers (e.g., LSODA[36] solvers). These computational programs have been largely used in the past.[30,37,38]

When mixtures with more than two/three independent components have been studied, simplifications have been normally introduced in the equations in order to keep the problem tractable. The most used of these approximations, the single file diffusion model, consists of supposing $Đ_{ij} = \infty$, thus making the B^{1-} matrix diagonal, with $Đ_i$ as diagonal elements. The effect of this approximation is discussed in the next sections.

In this paper, the numerical resolution of the system of PDEs reported in eq 29 is faced following a different approach; the aim is to have a method for the direct numerical resolution of the system of PDEs avoiding the symbolic inversion of the B matrix, thus allowing for the possibility to treat a generic number of components without introducing approximations in the equations. The price to pay for avoiding the symbolic inversion of the B matrix is a large number of numerical inversions of the same matrix. Both numerical and efficiency problems can originate from this choice, and this aspect is discussed at the end of this section. Obviously, the same problem is met in the Fick formulation if D is not supposed constant, and the algorithm presented hereafter can be applied also in this case. In this section, the numerical resolution of the MS equations is presented for the case where the unknown quantities are the molar fractions, but its extension to other cases (for instance, the coverage) is trivial.

In eq 29, D has a nonlinear dependence on all x_j, and this makes the numerical resolution of the equations problematic. First of all, D depends on z; second, and most important, it depends on the solutions of the set of differential equations. This problem is faced in this paper following two numerical approaches. The first is a finite difference approach already used by our group for the study of the salt diffusion in a solar pond[39−41] (SP) system, where the Fick diffusion coefficient D was position-dependent, given that it was a function of the salt concentration and of the temperature. Here, the derivation is more complex than that in the SP case due to the dependence of the flux of one chemical species on the concentration of all components. As in the SP case, the simple Crank−Nicolson[33,34] approach, with a discretization of both the space and the time variables, has been considered. The second approach is based on the accurate BDF also known as Gear's method,[1] as implemented in the ODEPACK[2] package.

In both approaches, the molar fractions $x_i(z,t)$ are computed on a regular grid of points in z ($\{z_1, z_2, ..., z_{n_z}\}$, $z_{i+1} - z_i = \Delta z$) and in t ($\{t_1, t_2, ..., t_{n_t}\}$, $t_{i+1} - t_i = \Delta t$), t_{n_t} being the total simulation time. Indicating the length of the simulated spatial interval with δ, we assume $z_1 = 0$ and $z_{n_z} = \delta$. In order to solve eq 29, one has to define the initial conditions, that is, all $x_i(z_j,t_1)$, the molar fractions of all components at all grid points at the first time step. Moreover $x_i(z_1,t_k)$ and $x_i(z_{n_z},t_k)$ for all i and k are defined by the boundary conditions.

The central aspect for the resolution of eq 29 is to have the numerical values of the $D_{ii'}(z_j,t_k)$ matrix elements. To this aim, the first problem is that they are actually unknown, depending on the molar fractions at time t_k, that is, the solutions of the equations that one wants to solve. In order to circumvent this difficulty, two strategies can be followed:[42]

• The $D_{ii'}(z_j,t_k)$ are substituted by their values at time t_{k-1}. These values are known, given that they depend on the $x_i(z_j,t_{k-1})$. The use of the molar fractions of the previous time step is expected to be a good approximation, given that they normally show modest variation from one time step to the next one (actually, the time step must be chosen to satisfy this requirement in order to have good quality results).

• One can consider the first strategy as the first step in a procedure in which $D_{ii'}(z_j,t_k)$ is approached iteratively. Once the $x_i(z_j,t_k)$ are computed in the first iterative step, they are used to compute $D_{ii'}(z_j,t_k)$, and the solution of eq 29 gives the second approximation of the $x_i(z_j,t_k)$. The convergence is reached when $x_i(z_j,t_k)$ do not show variations between two iterative steps.

In the following, we drop the variable t_k for the D matrix elements, with the assumption that one of the two strategies reported above is used. In the actual applications reported in this paper, the first strategy has been considered. However, in both cases, the numerical expression of the B and Γ matrices can be easily obtained for a given grid point in z at the time t_k, and the B^{-1} matrix is computed on the same grid points by the numerical inversion of the B matrix, thus allowing for the computation of the D matrix. The inversion of the B matrix must be performed $\sim n_z \times n_t$ times, and this can be supposed to be quite a demanding task. The use of the very efficient Lapack library[43] has however kept the CPU time within an acceptable range for all of the practical applications described in this paper (see the General Considerations subsection). Moreover, one can reasonably expect the numerical inversion of the B matrix to be rather prone to numerical problems in some cases; again, in the practical applications reported in this paper, the approach here described has been found to be stable and robust.

Equation 29 presents a further difficulty due to the dependence of the D matrix elements on z. This problem is faced here within a classical strategy using a finite difference numerical approach (accurate to the second order in space) with an appropriate centering, obtaining

$$\frac{\partial x_i(z_j,t)}{\partial t} = \frac{1}{(\Delta z)^2}\sum_{i'=1}^{n-1}\{D_{j+1/2}^{ii'}[x_{i'}(z_{j+1},t) - x_{i'}(z_j,t)] + D_{j-1/2}^{ii'}[x_{i'}(z_{j-1},t) - x_{i'}(z_j,t)]\} \quad (32)$$

where

$$D_{j+1/2}^{ii'} = \frac{D_{ii'}(z_{j+1}) + D_{ii'}(z_j)}{2} \quad (33)$$

$$D_{j-1/2}^{ii'} = \frac{D_{ii'}(z_{j-1}) + D_{ii'}(z_j)}{2} \quad (34)$$

By noticing that the $x_i(z_j,t)$ are a set of functions of a single variable (t), eq 32 is a system of ordinary differential equations (ODE), which can be solved using very effective numerical methods. The transformation of the original system of PDEs, eq 29 in a system of ODEs through the discretization in the z dimension, is known as the method of lines.[32]

For the resolution of the system of ODEs (eq 32), two different numerical approaches have been considered. The first is the Crank−Nicolson[33,34] method, which has been implemented from scratch in our code and is described in detail hereafter. The second approach, the Gear's method, is more complex and effective; in this case, use has been made of the ODEPACK[2] collection of Fortran solvers by interfacing our code to the LSODE solver. The details of this solver are not reported here and can be found in the literature.[2] The availability of two different numerical approaches has been exploited for a coherence test of our code.

For the sake of conciseness, in the following, $x_{j,k}^i$ indicates $x_i(z_j,t_k)$, the molar fraction of component i at the jth grid point

in z and at the time t_k. Using this notation, in the semi-implicit Crank−Nicolson[33,34] scheme (accurate to the second order in time), eq 32 becomes

$$\frac{x^i_{j,k} - x^i_{j,k-1}}{\Delta t} = \frac{1}{2(\Delta z)^2}\sum_{i'=1}^{n-1} D^{ii'}_{j+1/2}[(x^{i'}_{j+1,k} - x^{i'}_{j,k}) + (x^{i'}_{j+1,k-1} - x^{i'}_{j,k-1})] + D^{ii'}_{j-1/2}[(x^{i'}_{j-1,k} - x^{i'}_{j,k}) + (x^{i'}_{j-1,k-1} - x^{i'}_{j,k-1})] \quad (35)$$

It is worth noticing that this computational scheme, being a finite difference semi-implicit model, is stable for any choice of the time step Δt and of the grid interval Δz.

Moving all terms depending on t_k to the left part of the equation and those depending on t_{k-1} to the right part, one has

$$x^i_{j,k} - K\sum_{i'=1}^{n-1} x^{i'}_{j-1,k}D^{ii'}_{j-1/2} + K\sum_{i'=1}^{n-1} x^{i'}_{j,k}(D^{ii'}_{j+1/2} + D^{ii'}_{j-1/2}) - K\sum_{i'=1}^{n-1} x^{i'}_{j+1,k}D^{ii'}_{j+1/2} = x^i_{j,k-1} + K\sum_{i'=1}^{n-1}[D^{ii'}_{j+1/2}(x^{i'}_{j+1,k-1} - x^{i'}_{j,k-1}) + D^{ii'}_{j-1/2}(x^{i'}_{j-1,k-1} - x^{i'}_{j,k-1})] \quad (36)$$

where

$$K = \frac{\Delta t}{2(\Delta z)^2} \quad (37)$$

For each time step, eq 36 is a system of linear equations of the type

$$\mathrm{AX} = \mathrm{C} \quad (38)$$

where X is a vector collecting all of the unknown $x^i_{j,k}$ (from 1 to $n_z - 2$, the $x^1_{j,k}$ with $2 \le j \le n_z - 1$, from $n_z - 1$ to $2(n_z - 2)$, the $x^2_{j,k}$ with $2 \le j \le n_z - 1$, etc.). Introducing the superindex ξ, which depends on the two indices i and j according to the relation

$$\xi = (i - 1) * (n_z - 2) + j - 1 \quad (39)$$

one can write

$$X_\xi = x^i_{j,k} \quad (40)$$

The C vector has the form

$$C_\xi = x^i_{j,k-1} + K\sum_{i'=1}^{n-1}[D^{ii'}_{j+1/2}(x^{i'}_{j+1,k-1} - x^{i'}_{j,k-1}) + D^{ii'}_{j-1/2}(x^{i'}_{j-1,k-1} - x^{i'}_{j,k-1})] \quad (41)$$

The A matrix has a more complex structure. In a compact form, one can write

$$A_{\xi,\xi'} = \begin{cases} 1 + K(D^{ii'}_{j+1/2} + D^{ii'}_{j-1/2}) & \text{if } i = i', j = j' \\ K(D^{ii'}_{j+1/2} + D^{ii'}_{j-1/2}) & \text{if } i \neq i', j = j' \\ -KD^{ii'}_{j-1/2} & \text{if } j = j' - 1 \\ -KD^{ii'}_{j+1/2} & \text{if } j = j' + 1 \\ 0 & \text{otherwise} \end{cases} \quad (42)$$

In more detail, A has a block structure ($(n - 1) \times (n - 1)$ blocks) where each block is a tridiagonal $(n_z - 2) \times (n_z - 2)$ square matrix.

Some elements of the A and C matrices are then modified according to the chosen boundary conditions. Two possibilities are considered here, that is, constant concentrations or vanishing fluxes. In the first case, one has to add to the C elements with ξ defined by $j = 2$ or $j = n_z - 1$ the terms $Kx^i(0)\sum_{i'=1}^{n-1} D^{ii'}_{j-1/2}$ for $j = 2$ or $Kx^i(\delta)\sum_{i'=1}^{n-1} D^{ii'}_{j+1/2}$ for $j = n_z - 1$, where $x^i(0)$ and $x^i(\delta)$ are the imposed concentrations of the ith component at $z = 0$ and δ, respectively. In the case of vanishing fluxes, the diagonal elements of the A matrix with ξ defined by $j = 2$ or $n_z - 1$ are modified by subtracting the term $K\sum_{i'=1}^{n-1} D^{ii'}_{j-1/2}$ for $j = 2$ or $K\sum_{i'=1}^{n-1} D^{ii'}_{j+1/2}$ for $j = n_z - 1$.

The system of linear equations can be solved very effectively using a mathematical library such as, considering, for instance, a FORTRAN implementation, the DGESV routine of the Lapack library.[43]

Finally, once the $x^i_{j,k}$ are obtained with one of the two numerical approaches (Crank−Nicolson or Gear), the flux of component i, $N^i_{j,k}$, can be computed using a finite difference approach

$$N^i_{j,k} = -c_t\frac{1}{\Delta z}\sum_{i'=1}^{n}[D^{ii'}_{j-1/2}(x^{i'}_{j,k} - x^{i'}_{j-1,k}) + D^{ii'}_{j+1/2}(x^{i'}_{j+1,k} - x^{i'}_{j,k})] \quad (43)$$

Summarizing, for each time step, the scheme to be followed is as follows:

• For each grid point in z, compute the B matrix (defined by the specific problem considered), its inverse B^{-1}, and the product $\mathrm{B}^{-1}\Gamma$, thus obtaining the D matrix.

• Compute all of the values $x^i_{j,k}$ by using one of the two options, build the A matrix (eq 42) and the C vector (eq 41) and solve the system of linear eq 38 (Crank−Nicolson) or call the LSODE solver (Gear).

• Compute the fluxes.

This method is applied in the next sections in actual calculations on various problems.

Testing Examples and Applications

General Considerations. In the simulation of the diffusion process governed by the MS equations, it is useful to introduce a new set of units, as described for instance in a paper by Loos et al.[44]

In these units, the length of the studied system, δ, is the length unit and the lower single species MS diffusivity, $Đ_i^{\min}$ is the diffusivity unit. Within this unit system, time is expressed in units of $\delta^2/Đ_i^{\min}$.

All calculations have been performed on a Toshiba Laptop with an Intel Pentium 2.0 GHz CPU running the Linux operating system. The program has been compiled with the g95 compiler. The running time for a simulation calculation ranges from a

TABLE 1: Acetone and Methanol Diffusing through Stagnant Air in a Stefan Tube: Experimental and Optimized Input Parameters and Experimental and Computed Acetone and Methanol Fluxes[a]

parameter	experimental[b]	modified[b]	optimized[c,d]	optimized[c,e]
$Đ_{12}$	8.48×10^{-6}[f]			3.891×10^{-6}
l	0.2425	0.2380	0.23131	0.23131
x_1	0.3173[g]	0.319	0.30273	0.30235
x_2	0.5601[g]	0.528	0.53718	0.53757
$\tilde{N}_1$	1.779×10^{-3}	1.781×10^{-3}	1.719×10^{-3}	1.755×10^{-3}
$\tilde{N}_2$	3.121×10^{-3}	3.186×10^{-3}	3.281×10^{-3}	3.189×10^{-3}

[a] x_1 and x_2 are the molar fractions of acetone and methanol at the vapor−liquid interface. $Đ_{13}$ and $Đ_{23}$ are kept constant at the experimental value. The length is in m, fluxes are in mol m^{-2} s^{-1}, and diffusivities are in m^2 s^{-1}. [b] Carty and Schrodt.[25] [c] This work. [d] First set of optimized parameters. [e] Second set of optimized parameters. [f] Calculated using the method of Bae and Reed[50] (see Carty and Schrodt[25]). [g] Vapor−liquid equilibrium data.[47]

few seconds to a few hours, following the number of components, grid points, time steps, and the numerical approach used.

The results are always reported for the Crank−Nicolson method; the Gear one gives values which are practically identical (indistinguishable on the scale used in the figures).

Diffusion in the Bulk Fluid Phase: Acetone and Methanol Diffusing through Stagnant Air. In 1975, Carty and Schrodt[25] (CS) presented an experimental study in which a gas mixture of acetone and methanol was diffusing in a Stefan tube through stagnant air. This study has been already used for the validation of methods for the numerical resolution of the MS equations.[45,46] Here, besides its use as a first test for the numerical approaches presented in the previous section, some new considerations on this system are reported. In the following, the subscripts 1, 2, and 3 indicate acetone, methanol, and air, respectively. In the study of CS,[25] air was considered as a pure component since the diffusivities of acetone and methanol in oxygen and nitrogen are very similar. In the experimental setup, at the bottom of the tube, a film of a liquid mixture of acetone and methanol continuously flowed, so that the gas-phase concentrations close to the liquid−gas interface were considered constant. From the vapor−liquid equilibrium data of Freshwater and Pike,[47] the gas molar fractions were estimated to be $x_1 = 0.3173$, $x_2 = 0.5601$, and $x_3 = 0.1227$. At the top of the tube, a stream of dried air swept away the vapors of acetone and methanol, so that $x_1 = 0$, $x_2 = 0$, and $x_3 = 1.0$. The temperature was 328.5 K and the pressure 745.2 mm of Hg, and along the tube (0.2425 m long), air was stagnant. At the steady state, the measured fluxes were 1.779×10^{-3} mol m^{-2} s^{-1} for acetone and 3.121×10^{-3} mol m^{-2} s^{-1} for methanol. The experimental value of the diffusivities at constant temperature (328 K) and pressure (1 atm) of acetone (13.72×10^{-6} m^2 s^{-1}) and of methanol (19.91×10^{-6} m^2 s^{-1}) in air were taken from the literature.[48,49] The diffusivity of acetone in methanol was not experimentally available and was estimated to be 8.48×10^{-6} m^2 s^{-1}. The values of these parameters are reported in Table 1. The concentration of the various species was measured at seven points along the tube and are reported in Figure 1.

For this system the MS equations can be integrated at the steady state, obtaining the concentration profiles (see eqs 2 and 3 of CS[25]) as functions of the (constant) fluxes, of the diffusivities, and of the experimental concentrations at a chosen height of the tube. Carty and Schrodt noted that if the concentrations of the vapor−liquid interface are chosen as the known values, the concentration profiles show quite a large dependence on the used values. By using for all quantities the values reported above, a marked disagreement of the computed concentrations with respect to the experimental ones was observed.

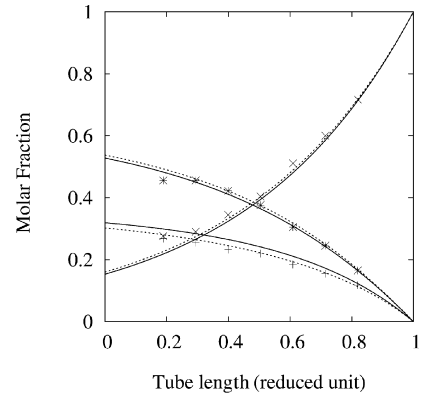

Figure 1. Acetone and methanol diffusing through stagnant air in a Stefan tube: experimental and optimized molar fraction profiles; +, ∗, and × symbols represent experimental points for acetone, methanol, and air, respectively. Full line: analytic solution with a set of modified parameters.[25] Dashed line: computed values with the second set of optimized parameters (this work; see Table 1).

The agreement between theory and experiment was improved[25] by modifying, in the computational input, the concentrations at the vapor−liquid interface ($x_1 = 0.319$, $x_2 = 0.528$, and $x_3 = 0.153$), the tube length ($l = 0.238$ m), and the fluxes ($N_1 = 1.781 \times 10^{-3}$ and 3.186×10^{-3} mol m^{-2} s^{-1}), while the diffusivities and the concentrations at the top of the tube were kept unchanged. The analytic molar fractions profiles with these parameters are also reported in Figure 1.

In both of the numerical approaches reported in this work, only the diffusivities and the concentrations at the top and the bottom of the tube must be defined. The time evolution of the concentration profiles is computed, and the steady state is reached when fluxes are constant along the tube. Our numerical approaches have been tested using the modified parameters used in CS[25] (also reported in Table 1) with $n_z = 101$ and $n_t = 10001$ and for a total simulation time of 5000 s (which ensures that the steady state is reached). The concentration profiles, and the fluxes (the output of our code) are practically indistinguishable from the analytic solution.

In order to verify if the parameter modification[25] gives the best agreement with the experimental data, a full optimization of a selected number of input parameters is here presented. The optimization is performed minimizing a function $f(\eta_1, \eta_2, ..., \eta_m)$, where $\eta_1, \eta_2, ..., \eta_m$ are the m parameters to be optimized. The function f can be defined in different ways; here, we use the form

$$f(\eta_1, \eta_2, ..., \eta_m) = \sum_{i=1}^{n-1} \sum_{j=1}^{n_{exp}} \left(\frac{\tilde{x}^i(\bar{z}_j) - \bar{x}^i(\bar{z}_j)}{\bar{x}^i(\bar{z}_j)} \right)^2 + 7 \sum_{i=1}^{n-1} \left(\frac{\tilde{N}_i - \bar{N}_i}{\bar{N}_i} \right)^2 \quad (44)$$

where $\bar{z}_j$ are the positions (in number $n_{exp} = 7$) along the tube at which the ith concentration, $\bar{x}^i(\bar{z}_j)$, has been measured and $\tilde{x}^i(\bar{z}_j)$ are the steady-state computed concentrations at the same positions. Analogously, $\tilde{N}_i$ and $\bar{N}_i$ are the steady-state computed and measured fluxes, respectively. The different weight on the fluxes with respect to the concentrations (7 versus 1) has been introduced in order to account for the larger number of measured

concentrations with respect to the number of measured fluxes. The minimization of $f(\eta_1, \eta_2, ..., \eta_m)$ has been conducted using the MINUIT[51,52] library developed at CERN.

Two sets of optimization parameters have been considered; the first contains the parameters modified in CS,[25] that is, the acetone and methanol concentrations at the vapor−liquid interface and the tube length l. The second set contains, besides the parameters of the first set, the acetone−methanol diffusivity, $Đ_{12}$, whose value in the original work[25] was theoretically estimated.

The optimized parameters for both sets are reported in Table 1. For the first set, they closely resemble the modified parameters defined in CS[25] (l being slightly lower, while the acetone and methanol concentrations are slightly lower and higher, respectively). The agreement with the experimental concentration is improved at the price of a slight worsening of the agreement of the computed fluxes with the experimental one. For the second set of parameters, one notes an almost negligible variation of the optimal parameters in common with the first set and a marked variation of the new parameter, $Đ_{12}$, which is less than one-half of the value estimated in the original work.[25] This modification brings about an improvement of the computed results, both for the concentrations and for the fluxes (in particular, for the methanol flux). The computed concentrations with the second set of parameters are shown in Figure 1, those corresponding to the first set of parameters being very close to them (they are not shown for the sake of clarity). With these parameters, the description of the experimental system can be considered very satisfactory.

Diffusion in Micropores: Transient Uptake of Mixture Components in Microporous Sorbents. The uptake process of two-component gas mixtures in microporous sorbents has a practical importance in particular in the field of separation science and for conversion processes. A transient numerical study of such a process was published in 1992 by Loos et al.,[44] with a numerical method different from the one reported in this paper. This method was developed for the study of a two-component system, and it is not straightforwardly generalizable to a generic number of components. In order to validate our numerical approach, the simulations presented by Loos et al.[44] are reproduced in this subsection. It is worth noticing that in the original work,[44] use has been made of the equations derived in a previous paper,[53] in which the B matrix in the Maxwell−Stefan formulation has an expression different from the one reported here (compare eqs 21 and 22 of the paper of Krishna[53] with eqs 25 and 26 of this paper). In order to make the comparison meaningful, the following simulations are performed with the definition of the B matrix reported by Krishna.[53]

The transient uptake of a binary mixture has been reported in Figure 2 of Loos et al.[44] for the case of three different diffusivity ratios $Đ_1^s/Đ_2^s$ (2, 10, and 100). The initial condition is vanishing concentrations in the microporous sorbent, while the boundary conditions are, at all time steps, constant fractional occupancy at one surface ($\theta_{1,k}^1 = 0.10$ and $\theta_{1,k}^2 = 0.85$) and vanishing fractional occupancy derivatives, that is, vanishing fluxes, at the other surface.

The uptake values as a function of time are reported in Figure 2, and the comparison with Figure 2 of Loos et al.[44] shows an excellent agreement of the two numerical methods.

Figure 3 reports a detailed analysis of the fractional occupancy profiles at various times (0.001, 0.01, 0.2, 0.4, 0.6, 0.8, 1.0, and 1.2 reduced units) for $Đ_1^s/Đ_2^s = 100$, allowing for a direct comparison with Figure 5 of Loos et al.;[44] the agreement is, also in this case, good.

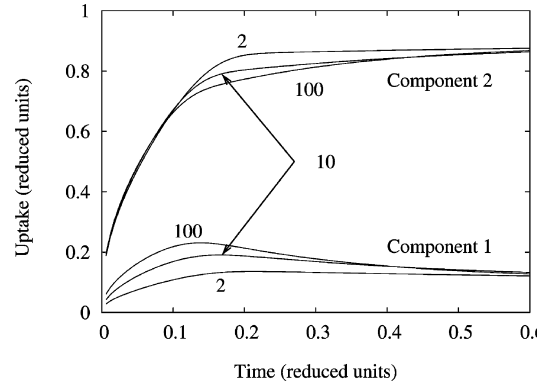

Figure 2. Uptake of a binary mixture on a microporous material as a function of time with the same conditions used for Figure 2 of Loos et al.[44] Number of grid points in z, $n_z = 21$; number of time steps, $n_t = 10000$. The numbers close to the curve represent the $Đ_1^s/Đ_2^s$ ratio used in the simulation (2, 10, 100).

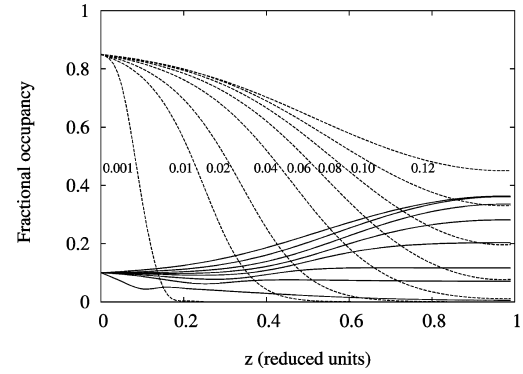

Figure 3. Uptake of a binary mixture on a microporous material. Occupancy profiles at various simulation times. Same conditions as those used for Figure 5 of Loos et al.[44] Number of grid points in z, $n_z = 21$; number of time steps, $n_t = 60000$. Full lines, component 1; dashed lines, component 2.

Diffusion in Micropores: Transient Permeation of a Binary Mixture through Zeolite Membranes. As a final test example, the transient permeation of a binary mixture through zeolite membranes has been considered. All simulated cases have been taken from Martinek et al.[54] (MGNF), with which the present results are compared. In MGNF,[54] as normally done in the literature, the numerical approach starts by the derivation of the analytic expression of the elements of the B^{-1} matrix. As previously commented, despite the efficiency of such an approach for a binary mixture, its implementation is difficult for a three-component system, and it is almost impossible for a generic number of components.

In the first simulation, the results reported in Figure 1 of MGNF[54] have been reproduced and are shown (on the same scale) in Figure 4, where the feed and permeate fluxes are reported for component 1 (faster-diffusing, upper part) and component 2 (slower-diffusing, lower part) as a function of time. The simulation parameters are here reported for the sake of completeness, $Đ_1^s = 5 \times 10^{-9}$ m^2 s^{-1}, $Đ_2^s = 1 \times 10^{-10}$ m^2 s^{-1}, $q_1^{sat} = q_2^{sat} = 2$ mol kg^{-1}, $\delta = 100$ μm, $\rho = 1800$ kg m^{-3}, $\theta_{1,k}^1 = \theta_{1,k}^2 = 0.33$, and $\theta_{n_z,k}^1 = \theta_{n_z,k}^2 = 0$. The cross diffusion coefficient $Đ_{12}^s$ has been computed from the single-component MS diffusivities using the logarithmic average

$$Đ_{ij}^s = (Đ_i^s)^{\theta_i/(\theta_i+\theta_j)}(Đ_j^s)^{\theta_j/(\theta_i+\theta_j)} \quad (45)$$

The parameters for the numerical simulation are 101 grid points in z and 50000 time steps.

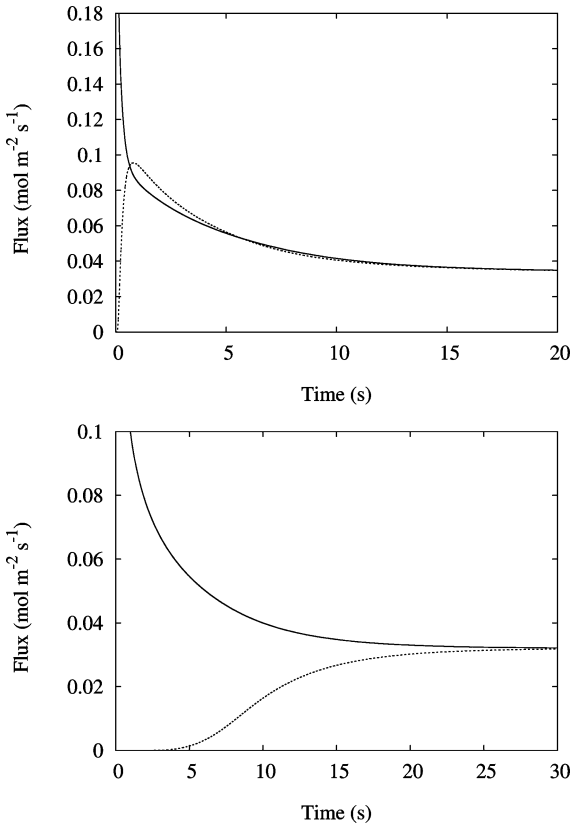

Figure 4. Feed (full line) and permeate (dashed line) fluxes of component 1 (upper part) and component 2 (lower part) as a function of time for the transient simulation of a permeation of a binary mixture through a zeolite membrane. The simulation parameters are the same as those used for Figure 1 of Martinek et al.[54] (see text for details).

The second simulation has been performed using the same parameters but considering $Đ^s_{12} = \infty$. The results are shown in Figure 5, where the feed and permeate fluxes for component 1 as a function of time (upper part) and the fractional occupancy of component 1 as a function of z for different times (lower part) are reported, allowing for a meaningful comparison with Figure 4 of MGNF.[54]

The agreement of the results here obtained with those of MGNF[54] is excellent.

Single-File Diffusion Model: An Example of the Effect of This Approximation. In some cases (as, for instance, with more than two independent components), approximations have been proposed in order to simplify the MS equations and to allow for a handy resolution of them. An example can be found in the paper of Krishna and van de Broeke[55] (KvB), where two approximations are considered, (1) the "single file diffusion model" (SFDM) where $Đ^s_{ij} = \infty$; the B^{-1} matrix is diagonal, with the $Đ^s_i$ as diagonal elements; and (2) the "constant Fick model"; the Fick matrix, D, is supposed to be coverage-independent. A special case of this approximation is that in which D is diagonal, with $Đ^s_i$ as diagonal elements. In this case, beyond the approximations introduced in the SFDM, the Γ matrix is supposed to be the identity matrix.

These approximations have been used in KvB[55] for the simulation of the permeation of different binary mixtures across a microporous membrane. Here, we concentrate our attention on two problems, both treated in the frame of the SFDM, the permeation of a propene(1)/propane(2) binary mixture across a silicalite membrane and the permeation of methane(1)/*n*-butane(2) binary mixture across a silicalite-1 membrane. The

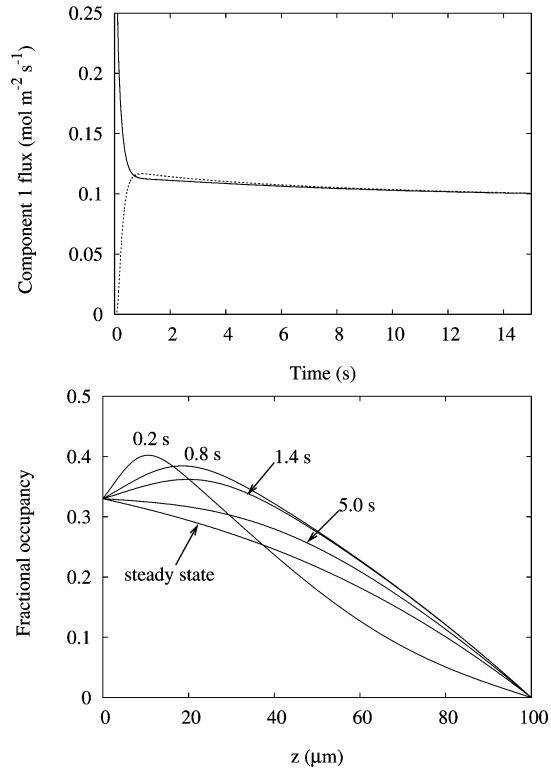

Figure 5. Feed (full line) and permeate (dashed line) fluxes of component 1 as a function of time (upper part) and fractional occupation of component 1 as a function of z at different times (lower part) for the transient simulation of a permeation of a binary mixture through a zeolite membrane. The simulation parameters are the same as those used for Figure 4 of MGNF[54] (see text for details).

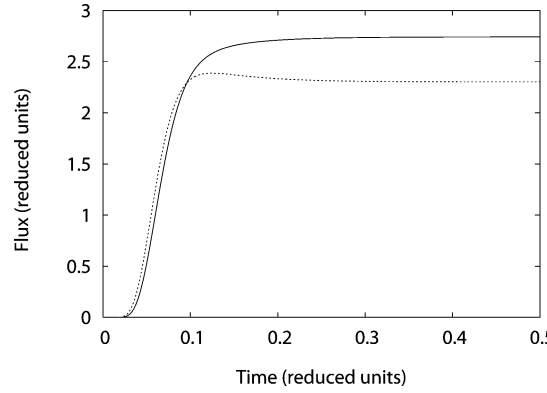

Figure 6. Permeate fluxes (full line, component 2; dashed line, component 1) of a propene(1)/propane(2) binary mixture across a silicalite membrane, using the SFDM. The simulation parameters are those of Figure 6 of KvB[55] (see text for details), 101 grid points in z, 50000 time steps.

permeate fluxes for both components as a function of time are reported in Figures 6 and 9 of KvB.[55]

In order to study the effect of the approximations introduced in the SFDM, we first tried to reproduce the results of KvB,[55] using the same simulation parameters, here summarized for the sake of completeness. For Figure 6 of KvB,[55] the boundary conditions are $\theta^1_{1,k} = 0.4183$ and $\theta^2_{1,k} = 0.5730$ at the feed interface and $\theta^1_{n_z,k} = 0$ and $\theta^2_{n_z,k} = 0$ at the permeate interface, while the MS diffusivity ratio is $Đ^s_2/Đ^s_1 = 1.15$. For Figure 9 of KvB,[55] the boundary conditions are $\theta^1_{1,k} = 0.2262$ and $\theta^2_{1,k} = 0.4762$ at the feed interface and $\theta^1_{n_z,k} = 0$ and $\theta^2_{n_z,k} = 0$ at the permeate interface, while the MS diffusivity ratio is $Đ^s_2/Đ^s_1 = 10$. The results of our simulations are reported in Figurse 6 and 7.

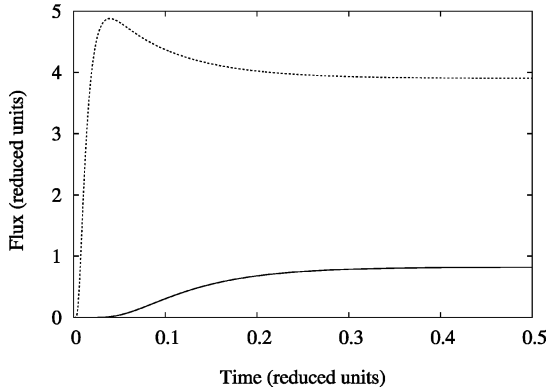

Figure 7. Permeate fluxes (full line, component 2; dashed line, component 1) of a methane(1)/*n*-butane(2) binary mixture across a silicalite-1 membrane, using the SFDM. The simulation parameters are those of Figure 9 of KvB[55] (see text for details), 101 grid points in z, 50000 time steps.

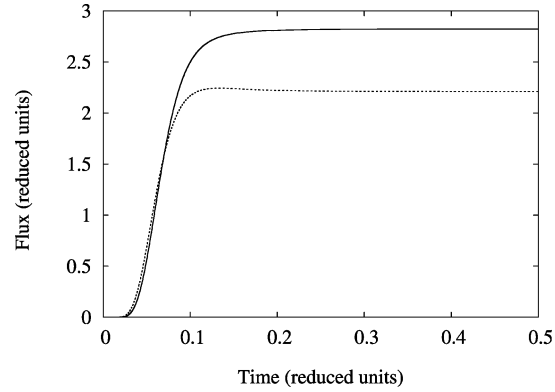

Figure 8. Permeate fluxes (full line, component 2; dashed line, component 1) of a propene(1)/propane(2) binary mixture across a silicalite membrane, for the case of finite $Đ_{ij}^{s}$ (computed from eq 45). The simulation parameters are those of Figure 6 of KvB[55] (see text for details), 101 grid points in z, 50000 time steps.

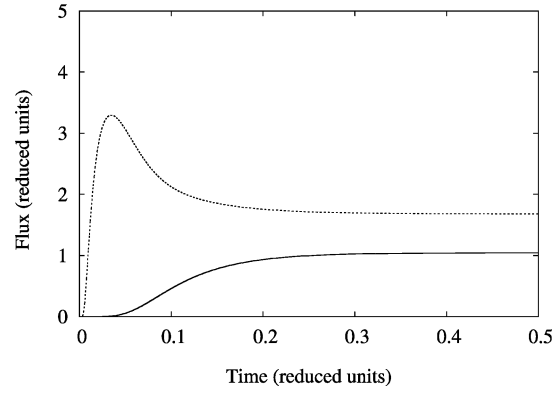

Figure 9. Permeate fluxes (full line, component 2; dashed line, component 1) of a methane(1)/*n*-butane(2) binary mixture across a silicalite-1 membrane, for the case of finite $Đ_{ij}^{s}$ (computed from eq 45). The simulation parameters are those of Figure 9 of KvB[56] (see text for details), 101 grid points in z, 50000 time steps.

The comparison with the results of KvB[55] shows that the present approach gives slightly different results for the first simulated system (the fluxes of both components being slightly higher in our calculation), while for the second system, the difference is marked, with even a different qualitative behavior (in KvB,[55] the flux of component 1 is lower than the flux of component 2, while the opposite happens in our calculations).

The results here obtained are confirmed by the analytic expression for the steady-state fluxes presented by Krishna and Baur[26] (eq 37 in their paper), which holds in the "weak confinement" regime (the MS diffusivities $Đ_i^{s}$ are not dependent on the factional occupancies), the one here considered. Using the reduced units, this equation can be written in the simplified form

$$\mathrm{N} = \frac{\ln(\theta_{n_z}^{\mathrm{V}}/\theta_1^{\mathrm{V}})}{1/\theta_1^{\mathrm{V}} - 1/\theta_{n_z}^{\mathrm{V}}}\mathrm{B}^{-1}\Delta\pi \qquad (46)$$

where B^{-1} is diagonal with elements $(B^{-1})_{11} = 1.15$ and $(B^{-1})_{22} = 1.00$. Moreover, $\Delta\pi_i = b_i(p_i(0) - p_i(\delta))$, where b_i, $p_i(0)$, and $p_i(\delta)$ are the parameter of the extended Langmuir isotherm, the partial pressure of component i at the feed interface, and that at the permeate interface, respectively (see KvB[55]). From eq 46, one has for the first system (Figure 6) $N_1 = 2.3015$ and $N_2 = 2.7416$, in excellent agreement with the steady-state values obtained by our numerical simulation (2.3023 and 2.7419, respectively).

The application of eq 46 to the second system (Figure 7) gives $N_1 = 3.9029$ and $N_2 = 0.8217$, also in this case in excellent agreement with those obtained by our numerical simulation (3.9047 and 0.8196, respectively).

The difference between the present results and those in the literature is probably due to a misprint of some of the input parameters in the captions of Figures 6 and 9 of KvB.[55] As said, the aim of this subsection is to show an example of the effect of the SFDM approximation and not to accurately describe a particular system. The problem of the permeation of a methane/*n*-butane mixture across a silicalite membrane has been faced by Krishna and collaborators in three subsequent papers,[56−58] where a more refined model of the adsorption isotherm has been considered, obtaining good agreement with the experimental results of Bakker.[59] The implementation in our code of adsorption isotherms different from the extended Langmuir one is under development.

The effect of the approximations introduced in the SFDM is clear by comparing Figures 6 and 7 with the results obtained for the case of finite $Đ_{ij}^{s}$ (computed from eq 45) reported in Figures 8 and 9.

One sees that in the first simulated case (propene/propane, Figures 6 and 8), the use of the SFDM leads to modest variations in the computed fluxes, slightly increasing the flux of the fast component (1) and decreasing that of the slow component (2). On the contrary, in the second simulated case (methane/*n*-butane, Figures 7 and 9), the change is marked. While the flux of the slower component (2) is only slightly reduced upon passing from the full treatment to the SFDM, the flux of the faster component is more than doubled.

The behavior found in the simulations based on SFDM can be easily understood; in the MS formulation, each component exerts a friction force on the other components,[3] and this force is proportional to the velocity difference of the components and to $(Đ_{ij}^{s})^{-1}$. In the SFDM, the friction forces are set to zero ($Đ_{ij}^{s} = \infty$). Such a friction force clearly reduces the velocity difference with respect to the case where it is absent, slowing down the faster species and speeding up the slowest species. The modifications introduced by the SFDM are obviously larger if the two components have very different MS diffusivities, $Đ_i^{s}$ (that is, in average, larger velocity differences).

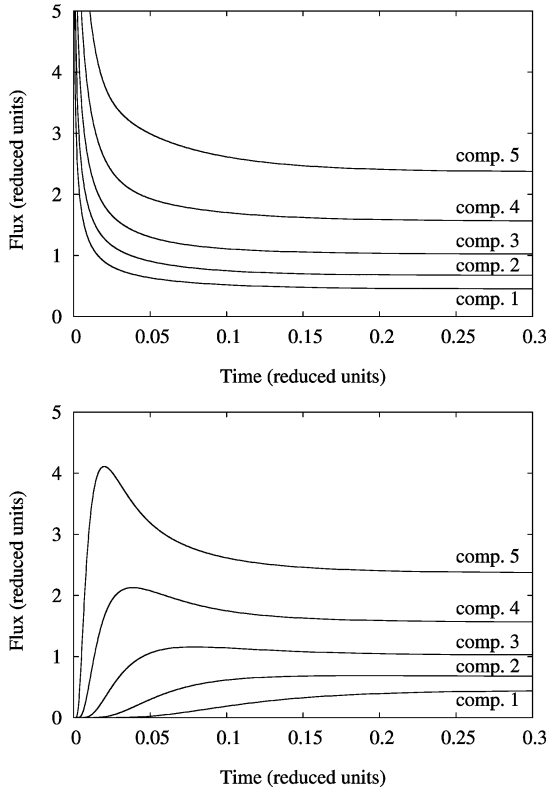

Figure 10. Transient permeation through a microporous membrane of a five-component mixture in the weak confinement scenario (see text); feed (upper part) and permeate (lower part) fluxes of the five components as a function of time. The MS diffusivities are defined by $Đ^s_{i+1}/Đ^s_i = 2$, with $Đ^s_{ij}$ computed from eq 45. Boundary conditions: $\theta^i_{1,k} = 0.15$ and $\theta^i_{n_z,k} = 0$ at the feed and permeate interfaces, respectively.

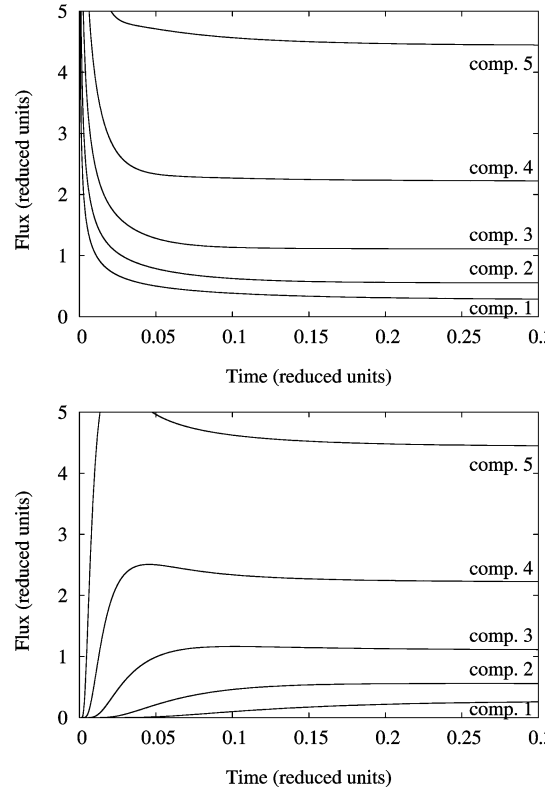

Figure 11. Transient permeation through a microporous membrane of a five-component mixture in the weak confinement scenario (see text); feed (upper part) and permeate (lower part) fluxes of the five components as a function of time. The MS diffusivities are defined by $Đ^s_{i+1}/Đ^s_i = 2$ and $Đ^s_{ij} = \infty$ (SFDM). Boundary conditions: $\theta^i_{1,k} = 0.15$ and $\theta^i_{n_z,k} = 0$ at the feed and permeate interfaces, respectively.

Finally, let us treat the case in which the Fick matrix D is considered diagonal and constant with $Đ^s_i$ as diagonal elements (the Γ matrix is the identity matrix). In the systems here studied, this approximation corresponds to consider as the constant D matrix that computed at the permeate interface (where the Γ matrix is the identity matrix) in the SFDM. For the first system here considered at the steady state, the fluxes are $N_1 = 0.48$ and $N_2 = 0.57$, to be compared with $N_1 = 2.30$ and $N_2 = 2.74$ computed with the SFDM (see Figure 6). For the second system, the steady-state fluxes are $N_1 = 2.26$ and $N_2 = 0.48$ ($N_1 = 3.90$ and $N_2 = 0.82$ in the SFDM; see Figure 7). In both cases, one observes a marked reduction of the fluxes.

Multicomponent Transient Permeation through a Microporous Membrane: Results for a Five-Component Mixture. In order to show the capability of the numerical approaches here reported to treat the one-dimensional diffusion problem with the MS formulation for more than two independent components (more than two components for surface diffusion; more than three components in bulk diffusion), some results are here presented for the transient permeation of a mixture of five components through a microporous membrane in a model system.

The model system can be seen as a multicomponent generalization of the results presented in MGNF[54] for a binary mixture. The simulation starts with an empty microporous membrane, and the boundary conditions are constant fractional occupancies at both membrane interfaces. A feed gas mixture with five components (with constant partial pressures) is in contact with the microporous membrane, and the fractional occupancies on the feed interface are equal for all components, $\theta^i_{1,k} = 0.15$. On the permeate interface, the fractional occupancies are all vanishing, $\theta^i_{n_z,k} = 0$. The MS diffusivities are chosen to satisfy the ratio $Đ^s_{i+1}/Đ^s_i = 2$. All simulations described in this section have been performed with 101 grid points in z and 50000 time steps.

The fluxes as functions of time are reported in Figure 10 for the case in which the MS diffusivities are independent of loading, while the $Đ^s_{ij}$ are defined by eq 45.

The feed fluxes do not show a particular behavior; the shape is roughly the same for all components, the steady-state fluxes being related to the MS diffusivities. On the contrary the permeate fluxes have a different qualitative profile for the various components. The permeate flux profiles for components 5 (the faster diffusion species) and 1 (the slower one) closely resemble those reported in Figure 4 for the two components of a binary mixture. The other three components show intermediate profiles, with a gradual variation between the two limiting cases. It is interesting to note that, as found for binary mixtures,[54] the flux for the slower component evolves as expected for a single-component diffusion, while the flux of the faster component has a qualitatively different shape, with a marked overshoot of the steady-state flux in the initial part of the simulation and then a monotonic decreasing of the flux toward the steady-state flux.

In a second simulation, the SFDM ($Đ^s_{ij} = \infty$) has been applied while keeping the other physical and numerical parameters unchanged. From the flux profiles reported in Figure 11, one notes that the use of the SFDM does not strongly modify the qualitative behavior of the system, while from the quantitative point of view, the faster species (components 4 and 5) have increased their fluxes and the slower species (components 1 and

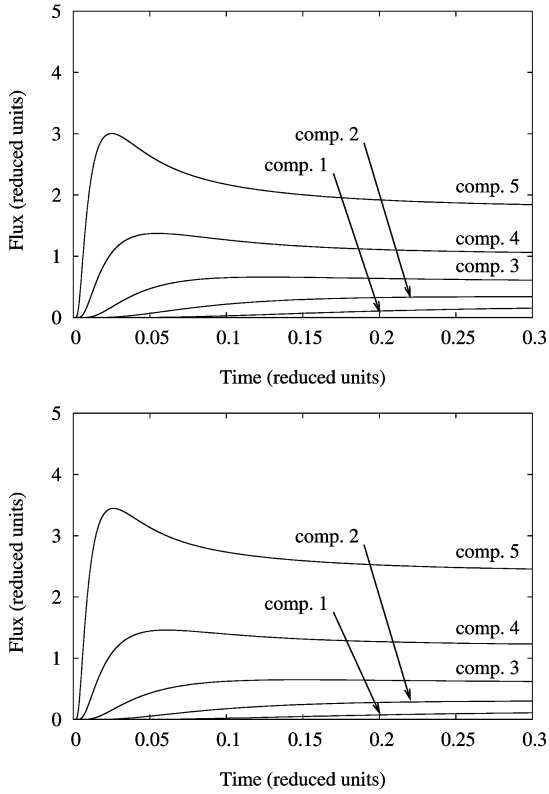

Figure 12. Transient permeation through a microporous membrane of a five-component mixture in the strong confinement scenario (see text). Feed fluxes of the five components as a function of time for the case in which $Đ_{ij}^{s}$ are computed from eq 45 (upper part) and that in which $Đ_{ij}^{s} = \infty$ (lower part) are shown. The MS diffusivities are defined by $Đ_{i+1}^{s}/Đ_{i}^{s} = 2$. Boundary conditions: $\theta_{1,k}^{i} = 0.15$ and $\theta_{n_c,k}^{i} = 0$ at the feed and permeate interfaces, respectively.

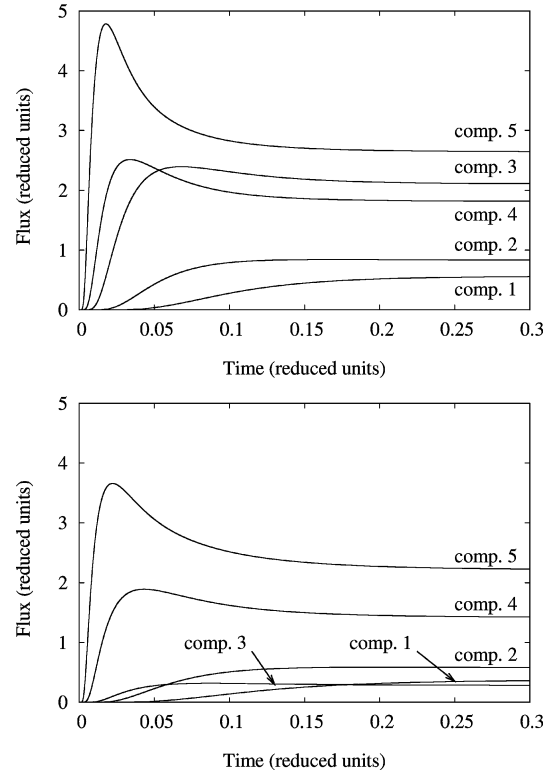

Figure 13. Transient permeation through a microporous membrane of a five-component mixture in the strong confinement scenario (see text). Feed fluxes of the five components as a function of time for $\theta_{1,k}^{3} = 0.25$ (upper part) and $\theta_{1,k}^{3} = 0.05$ (lower part) as boundary condition on the feed membrane surface are shown. The other boundary conditions are $\theta_{1,k}^{1} = \theta_{1,k}^{2} = \theta_{1,k}^{4} = \theta_{1,k}^{5} = 0.15$ for the feed surface and $\theta_{n+z,k}^{i} = 0$ for the permeate surface. The MS diffusivities are defined by $Đ_{i+1}^{s}/Đ_{i}^{s} = 2$ and $Đ_{ij}^{s}$ computed from eq 45.

2) have reduced their fluxes. Component 3 has roughly the same flux as that in Figure 10. The values of the steady-state fluxes in the numerical simulation have been confirmed by the agreement with the results of the analytic solution (eq 37 of Krishna and Baur[26]) for the weak confinement scenario ($Đ_{i}^{s}$ independent of loading) for which the formula is exact (while it is only approximate for $Đ_{ij}^{s}$ defined by eq 45).

Previous studies have shown that the hypothesis that the $Đ_{i}^{s}$ are independent of loading is often wrong, in particular, with high fractional occupancy. The dependence of $Đ_{i}^{s}$ on the loading can be complex.[60−62] However, in many cases, a linear dependence of $Đ_{i}^{s}$ on the total fractional occupancy, $\theta = \sum_{i}^{n} \theta_{i}^{s}$, has been observed (see Krishna and Baur[26])

$$Đ_{i}^{s}(\theta) = Đ_{i}^{s}(0)(1 - \theta) \tag{47}$$

and this is called the "strong confinement scenario". A simulation based on this definition of the MS diffusivities (the other parameters being those used for Figure 10) has been performed. The permeate fluxes are reported in Figure 12 for the case in which $Đ_{ij}^{s}$ are computed from eq 45 (upper part) and for the SFDM (lower part).

The comparison with the permeate fluxes in the weak confinement scenario (Figures 10 and 11, lower part) shows that all fluxes are lower in the strong confinement scenario (as expected from the reduction of the MS diffusivities in the latter case). As in the preceding case, the use of the SFDM increases the fluxes of the fast-moving components 4 and 5 and reduces the fluxes of the tardy components 1 and 2, while the flux of component 3 remains almost unchanged. It is worth noticing that an analytic solution for the steady-state fluxes has been presented also in the case of the strong confinement scenario, and this solution is exact in the case of the SFDM (eq 44 in Krishna and Baur[26]). The results presented in the lower part of Figure 12 at long time agree with the values computed with the analytic equation.

Finally, the effect of the variation of one of the fractional occupancies (that of component 3, which has intermediate MS diffusivity) at the feed surface has been considered. All of the other parameters are those of the simulation reported in Figure 10. Figure 13 shows the permeate fluxes for the cases of $\theta_{1,k}^{3} = 0.25$ (upper part) and $\theta_{1,k}^{3} = 0.05$ (lower part), for the weak confinement scenario and with the logarithmic average definition of $Đ_{ij}^{s}$ (eq 45). One clearly sees that, with respect to the case with $\theta_{1,k}^{3} = 0.15$, the increase (reduction) of $\theta_{1,k}^{3}$ leads to an increase (reduction) of the flux of component 3 at all times. This has a consequence, even if quite modest, also on the other fluxes; in the first case, component 3 has a dragging effect, slightly increasing all fluxes, while in the second case, it has a slowing down effect, with a moderate reduction of all fluxes. Moreover, one notes an intensification or a reduction of the overshooting of the faster component flux with respect to the steady-state flux related to the increase or decrease of the fractional occupancies of component 3 on the feed surface.

For all cases considered in this section, the fluxes after 0.3 reduced units of time are reported in Table 2, together with the steady-state values computed with the analytic equations. It is worth noticing that in most cases, the steady state has not been reached in the simulations (the weak confinement case with the

TABLE 2: Permeate Fluxes (Reduced Units) after a Simulation Time of 0.3 Reduced Units for the Permeation through a Microporous Membrane of a Five-Component Mixture[a]

system	comp. 1	comp. 2	comp. 3	comp. 4	comp. 5
WC-LA[1]	2.38(2.21)	1.57(1.50)	1.03(1.02)	0.68(0.69)	0.44(0.46)
WC-LA[2]	2.65(2.54)	1.82(1.77)	2.11(2.10)	0.83(0.84)	0.56(0.57)
WC-LA[3]	2.23(2.04)	1.43(1.35)	0.28(0.28)	0.58(0.59)	0.36(0.39)
WC-SF[1]	4.45(4.44)	2.23(2.22)	1.11(1.11)	0.55(0.55)	0.26(0.28)
SC-LA[1]	1.84(1.20)	1.06(0.81)	0.61(0.55)	0.34(0.37)	0.15(0.25)
SC-SF[1]	2.45(2.40)	1.23(1.20)	0.62(0.60)	0.30(0.30)	0.11(0.15)

[a] Analytic values are within parentheses. The steady-state limit is only approached (in particular, for the simulations with low fluxes). WC, weak confinement; SC, strong confinement; LA, logarithmic average of $Đ_{ij}^{s}$; SF, single-file diffusion model.

SFDM being the closest to the steady state). Moreover, let us note that the analytic equations give exact values only for the SFDM, while if eq 45 is used for $Đ_{ij}^{s}$, they are only approximate.

The results discussed in this section, besides their interest for the comprehension of multicomponent diffusion, clearly show that the algorithm described in this paper can be successfully applied for the study of systems with more than two independent components.

Conclusions

This paper describes a new algorithm for the one-dimensional numerical resolution of the Maxwell−Stefan equations in the transient regime. The key points of this approach are:

• The MS equations are rewritten in the Fick-like form $N = -c_t D(\partial x/\partial z)$, where $D = B^{-1}\Gamma$ and B^{-1} and Γ depend on the specific problem under study.

• Both the spatial and the time variables are discretized on regular grids of points.

• The symbolic inversion of the B matrix is substituted by the numerical inversion of it on all grid points and at all time steps.

• The derivatives are evaluated with a second-order accurate in time Crank−Nicolson finite difference approach or using the Gear method as implemented in the ODEPACK package.

• For the Crank−Nicolson approach, the problem (including the definition of the boundary conditions) is reformulated in a matrix form, leading to a system of linear equations, which is solved using very efficient mathematical libraries.

The method has been applied to different systems, with the aim of verifying its correctness (by the comparison with previously published studies), and for new applications. The MS equations have been solved with the same computational code for the bulk diffusion, for the uptake process in a microporous material, and then for the permeation through microporous membranes, showing that the approach is general, stable, and solid. One of the innovative aspects of the present formulation is the possibility to treat a generic number of components, the limits being in the computational hardware. A second relevant aspect is related to possible future developments; indeed, the formulation here described allows for an easy modification of some assumptions for what concerns the key quantities such as, for instance, the adsorption isotherm in microporous surface diffusion, the dependence of the MS diffusivities on the fractional occupancies, or the nature of the $Đ_{ij}^{s}$ coefficients. Such a possibility, which depends on the fact that in the algorithm, the B^{-1} and Γ matrices are explicitly computed on the various grid points in z, can allow the use of various expressions for the relevant key quantities and even the use of experimental (known on a grid of points) data. The conjugation of these two innovative aspects makes this method interesting, besides its use for the simulation of the diffusion process in systems described by known models, also for testing new hypotheses on the key quantities or new models for the description of the diffusion processes at the molecular level in technologically relevant materials.

This paper reports, as an example of the potentials of the method, the study of the effect of some assumptions (weak/strong confinement, logarithmic average for the $Đ_{ij}^{s}$ or SFDM) and parameters (fractional occupancy of a given component at the feed surface) in the case of the transient permeation through a microporous membrane of a five-component mixture.

Two different numerical schemes have been implemented in our code, the simple Crank−Nicolson method and the more refined BDF or Gear's method. Even if the comparison of different ODEs solvers is not the subject of this paper, a short comment can be made. Both approaches have shown to be stable and robust, and they give pretty much the same results (small differences are due to the different integration schemes and are expected). Keeping in mind that the Crank−Nicolson method has been implemented from scratch (plausibly with only a partial optimization of the code) while the Gear method has been implemented by using the ODEPACK Fortran package (certainly written with a high level of optimization), our calculations have shown that the Gear method is superior and faster, in particular, for the system with a large number of components. Nevertheless, we plan to keep both methods in our code, given that they allow for a consistency check of the results.

Finally, it is worth noticing that the algorithm here described can be obviously used also for the resolution of the diffusion problem in the Fick formulation; actually, the MS equations are first brought back to Fick's formulation and then solved with the hypothesis that the Fick diffusivities are position-dependent. This possibility can be of interest in research fields not discussed here, such as, for instance, the crystal growth in protein solution[63] or solid−solid metallic diffusion,[64] where the Fick description of the diffusion process is normally used.

Acknowledgment. This work has been carried out within the FISR project "Sistemi integrati di produzione di idrogeno e sua utilizzazione nella generazione distribuita" and with the financial support of the University of Ferrara through its local funding. The authors wish to thank Lorenzo Pareschi for stimulating discussions on the numerical resolution of PDEs.

References and Notes

(1) Shampine, L. F.; Gear, C. W. *SIAM Rev.* **1979**, *21*, 1.
(2) Hindmarsh, A. C. *Serial Fortran Solvers for ODE Initial Value Problems*, Technical Report; **2006**; https://computation.llnl.gov/casc/odepack/odepack_home.html.
(3) Krishna, R.; Wesselingh, J. A. *Chem. Eng. Sci.* **1997**, *52*, 861.
(4) Amundson, N. R.; Pan, T. W.; Paulsen, V. I. *Fluid Mech. Transp. Phenom.* **2003**, *49*, 813.
(5) Kerkhof, P. J. A. M.; Geboers, M. A. M. *Chem. Eng. Sci.* **2005**, *60*, 3129.
(6) Gavalas, G. R. *Ind. Eng. Chem. Res.* **2008**, *47*, 5797.
(7) Duncan, J. B.; Toor, H. L. *AICHE J.* **1962**, *8*, 38.
(8) Maxwell, J. C. *Philos. Trans. R. Soc.* **1866**, *157*, 49.
(9) Stefan, J. *Sitzungsber. Akad. Wiss. Wien* **1871**, *63*, 63.
(10) Wang, Y.; LeVan, M. D. *J. Phys. Chem. B* **2008**, *112*, 8600.
(11) Mitrovic, J. *Int. J. Heat Mass Transfer* **1997**, *40*, 2373.
(12) Sircar, S.; Golden, T. C. *Sep. Sci. Technol.* **2000**, *35*, 667.
(13) Krishna, R.; van Baten, J. M. *Ind. Eng. Chem. Res.* **2006**, *45*, 2084.
(14) Do, H. D.; Do, D. D. *Chem. Eng. Sci.* **1998**, *53*, 1239.
(15) Hung, H. W.; Lin, T. F.; Baus, C.; Sacher, F.; Brauch, H. J. *Environ. Technol.* **2005**, *26*, 1371.
(16) Li, S.; Tuan, V. A.; Noble, R. D.; Falconer, J. L. *Environ. Sci. Technol.* **2003**, *37*, 4007.

(17) Hogendoorn, J. A.; van der Veen, A. J.; van der Stegen, J. H. G.; Kuipers, J. A. M.; Versteeg, G. F. *Comput. Chem. Eng.* **2001**, *25*, 1251.
(18) Lehnert, W.; Meusinger, J.; Thom, F. *J. Power Sources* **2000**, *87*, 57.
(19) Runstedtler, A. *Chem. Eng. Sci.* **2006**, *61*, 5021.
(20) Kaczmarski, K.; Cavazzini, A.; Szabelski, P.; Zhou, D.; Liu, X.; Guiochon, G. *J. Chromatogr., A* **2002**, *962*, 57.
(21) Banat, F. A.; Al-Rub, F. A.; Shannag, M. *Heat Mass Transfer* **1999**, *35*, 1432.
(22) No, H. C.; Lim, H. S.; Kim, J.; Oh, C.; Siefken, L.; Davis, C. *Nucl. Eng. Des.* **2007**, *237*, 997.
(23) Magin, T. E.; Degrez, G. *J. Comput. Phys.* **2004**, *198*, 424.
(24) Kolesnikov, A. F. *An efficient modeling stagnation point heat transfer for subsonic aerothermal test conditions*, Technical Note 196; Von Karman Institute for Fluid Dynamics: Chaussée de Waterloo, Belgium; 2001.
(25) Carty, R.; Schrodt, T. *Ind. Eng. Chem. Fundam.* **1975**, *14*, 276.
(26) Krishna, R.; Baur, R. *Chem. Eng. J.* **2004**, *97*, 37.
(27) Pisani, L. *Int. J. Heat Mass Transfer* **2008**, *51*, 650.
(28) Krishna, R. *Gas Sep. Purif.* **1993**, *7*, 91.
(29) Kapteijn, F.; Moulijn, J. A.; Krishna, R. *Chem. Eng. Sci.* **2000**, *55*, 2923.
(30) Krishna, R.; van Baten, J. M. *Microp. Mesop. Mat.* **2008**, *109*, 91.
(31) Matuszak, D.; Donohue, M. D. *Chem. Eng. Sci.* **2005**, *60*, 4359.
(32) Sciesser, W. E. *The numerical method of lines: integration of partial differential equations*; Academic Press: San Diego, CA, 1991.
(33) Crank, J.; Nicolson, P. *Adv. Comput. Math.* **1996**, *6*, 207.
(34) Press, W. H.; Flannery, B. P.; A., T. S.; T., V. W. *Numerical Recipes in FORTRAN 77: The Art of Scientific Computing*; Cambrige University Press: New York, 1992.
(35) Finlayson, B. *Nonlinear Analysis in Chemical Engineering*; McGraw-Hill Inc.: New York, 1980.
(36) Petzold, L. R.; Hindmarsh, A. C. *LSODA*, Technical Report; Lawrence Livermore National Laboratory: Livermore, CA; 1997.
(37) Delgado, J. A.; Rodigues, A. E. *Ind. Eng. Chem. Res.* **2001**, *40*, 2289.
(38) Sousa, J. M.; Mendes, A. *J. Membr. Sci.* **2004**, *243*, 283.
(39) Angeli, C.; Leonardi, E. *Int. J. Heat Mass Transfer* **2004**, *47*, 1.
(40) Angeli, C.; Leonardi, E. *Int. J. Heat Mass Transfer* **2005**, *48*, 4633.
(41) Angeli, C.; Leonardi, E.; Maciocco, L. *Solar Energy* **2006**, *80*, 1498.
(42) Samarskii, A. A. *The theory of difference schemes*; Marcel Dekker, Inc.: Basel, Switzerland, 2001; http://www.dekker.com.
(43) Anderson, E.; Bai, Z.; Bischof, C.; Blackford, S.; Demmel, J.; Dongarra, J.; Du Croz, J.; Greenbaum, A.; Hammarling, S.; McKenney, A.; Sorensen, D. *LAPACK Users' Guide*, Third Edition; Society for Industrial and Applied Mathematics: Philadelphia, PA, 1999.
(44) Loos, J.-P. W. P.; Verheijen, P. J. T.; Moulin, J. A. *Collect. Czech. Chem. Commun.* **1992**, *57*, 687.
(45) Chen, K. S.; Evans, G. H.; Larson, R. S.; Noble, D. R.; Houf, W. G. *Final report on LDRD project: A phenomenological model for multicomponent transport with simultaneous electrochemical reactions in concentrated solutions*, Technical Report; Sandia National Laboratories: Albuquerque, NM, 2000.
(46) Dilman, V. V. *Theor. Found. Chem. Eng.* **2008**, *42*, 166.
(47) Freshwater, D. C.; Pike, K. A. *J. Chem. Eng. Data* **1967**, *12*, 179.
(48) Richardson, J. F. *Chem. Eng. Sci.* **1959**, *10*, 234.
(49) Mrazek, R. V.; Wicks, C. E.; Prabhu, K. N. S. *J. Chem. Eng. Data* **1968**, *13*, 508.
(50) Bae, J. H.; Reed, T. M., III. *Ind. Eng. Chem. Fundam.* **1971**, *10*, 36.
(51) James, F.; Roos, M. *Comput. Phys. Commun.* **1975**, *10*, 343.
(52) James, F. *MINUIT, Function Minimization and Error Analysis*, CERN Program Library, D506; CERN Program Library Office: Geneva, Switzerland; http://cern.ch/wwwasdoc/minuit/minmain.html.
(53) Krishna, R. *Chem. Eng. Sci.* **1990**, *45*, 1779.
(54) Martinek, J. G.; Gardner, T. Q.; Noble, R. D.; Falconer, J. L. *Ind. Eng. Chem. Res.* **2006**, *45*, 6032.
(55) Krishna, R.; van de Broeke, L. J. P. *Chem. Eng. J.* **1995**, *57*, 155.
(56) Krishna, R. *Int. Commun. Heat Mass Transfer* **2001**, *28*, 337.
(57) Krishna, R.; Baur, R. *Sep. Purif. Technol.* **2003**, *33*, 213.
(58) Smit, B.; Krishna, R. *Chem. Eng. Sci.* **2003**, *58*, 557.
(59) Bakker, W. J. W. *Structured systems in gass separation*, Ph D. thesis, Delft University of Technology, 1999.
(60) Li, S.; Falconer, J. L.; Noble, R. D.; Krishna, R. *J. Phys. Chem. C* **2007**, *111*, 5075.
(61) Lee, S. C. *J. Membr. Sci.* **2007**, *306*, 267.
(62) Chmelik, C.; Heinke, L.; Kärger, J.; Schmidt, W.; Shash, D. B.; van Baten, J. M.; Krishna, R. *Chem. Phys. Lett.* **2008**, *459*, 141.
(63) Albright, J. G.; Annunziata, O.; Miller, D. G.; Paduano, L.; Pearlstein, A. J. *J. Am. Chem. Soc.* **1999**, *121*, 3256.
(64) Kulkarni, K. N.; Girgis, A. M.; Ram-Mohan, L. R.; Dayananda, M. A. *Philos. Mag.* **2007**, *87*, 853.

JP900760C